Design of Periodic Signals Using FM Sweeps and Amplitude Modulation for Ocean Acoustic Travel-Time Measurements

Shuozhong Wang, Mark L. Grabb, *Student Member, IEEE*, and Theodore G. Birdsall, *Member, IEEE*

Abstract— **A design procedure for an amplitude-modulated and nonlinear frequency-modulated (AM–NLFM) signal is introduced. The designed signal can drive a given transducer to its peak power to produce a sound pressure waveform into the water with a desired power spectrum and maximum possible energy. The signal can be formed either in the time domain or in the frequency domain. The frequency domain approach gives an output power spectrum precisely identical to a preferred shape. Therefore, the sidelobe levels after matched filtering are not raised by unwanted spectral magnitude ripples which exist when a time domain method is adopted. The absence of spectral ripples is desirable for applications requiring long range transmission and good multipath discrimination capability. An acceptable tradeoff between time resolution and sidelobe levels is achieved by properly choosing the desired power spectral shape. As the time resolution is usually the most critical specification for precision travel-time measurements, it is shown that by sacrificing some of the transducer's output power capability, a waveform with a considerably wider bandwidth can be transmitted, resulting in a significantly enhanced time resolution. A quasi-steady-state (QSS) approximation is used in the signal design, leading to a manageable and intuitive design procedure.**

I. Introduction

FOR long-range bistatic sound transmission through the ocean sound channel such as in ocean acoustic tomography [1], [2] and in acoustic thermometry of ocean climate (ATOC) [3], the signal used should allow sufficient sound energy delivery into the ocean so that the signal received at a long range, perhaps several megameters, has a sufficiently high signal-to-noise ratio. Therefore, precision measurements of sound travel time can be made, and a low rate of false alarm is attainable. Additionally, the signal should allow good time resolution after signal processing so that closely spaced arrivals due to multipath can be resolved. M sequences have been used successfully in previous experiments [1], [4]. An m sequence with a long codeword, therefore high signal-to-noise energy ratio per word, satisfies the long-range transmission requirement. The matched-filter output of such a signal has the same time resolution as a monopulse or periodic pulse system whose pulse width is one digit (bit) wide. The transducer determines the minimum pulse or digit duration achievable at high power. In other words, m sequences provide high signal energy by transmitting over a long time (large T) and good time resolution by using a sequence of short pulses (large W), thereby achieving a large TW product [5]. The transmission time T is not limited as with monostatic measurements since bistatic system receivers are distant from the transmitter, and the transmitter may continue to transmit while the receiver is receiving. However, for coherent processing, the total transmission time is limited by the maximum time that the medium will support coherent propagation.

Time-limited transmissions consisting of an integer number of replications of a basic signal play a special role in bistatic travel-time measurements that need to transmit more energy than can be sent in a short burst. With apologies to the purist, we call these multiperiod transmissions "periodic signals." The extraordinary properties of an m sequence are based on periodic measures; for example, the perfect autocorrelation function with zero beyond ± 1 digit delay obtained with matched phase modulation is a periodic m-sequence property. When the propagation causes multiple arrivals, one may transmit a periodic signal with period longer than the arrival span, and analyze a portion of the reception during which all arrivals are ever present. Said simply, the analyzed portion of the reception should be "steady state." The alternative to steady-state analysis is to analyze a time interval which includes all arrivals and necessarily includes some noise before the first arrival and after the last arrival.

The use of periodic signals has several advantages besides focusing on the steady-state reception. The discrete Fourier transform (DFT) is the mathematically appropriate spectral tool for a finite number of uniformly spaced samples, with the DFT size matched to an integer number of periods. (This is in contrast to approximate spectral methods that do not use matching eigenfrequencies.) The signal generator for these signals is a periodic discrete sequence of samples read from memory, D/A converted, and very mildly filtered, so the DFT is most appropriate. If the propagation is truly steady during the reception, "period summing" the reception to obtain a one-period representative for analysis is simple and ideal, and usually reduces subsequent processing time. If the propagation is slowly varying, the receiver may test integer-period subsets of the reception to determine the best subset size to sum, or

Manuscript received March 10, 1994; revised July 22, 1994. This work was supported by the Advanced Research Projects Agency (ARPA) on the project Acoustic Thermometry of Ocean Climate (ATOC).

S. Wang was on leave at the Department of Electrical Engineering and Computer Science, University of Michigan, Ann Arbor, MI 48109. He is with the Department of Telecommunications and Electronic Engineering, Shanghai University, Shanghai 200072, People's Republic of China.

M. L. Grabb and T. G. Birdsall are with the Department of Electrical Engineering and Computer Science, University of Michigan, Ann Arbor, MI 48109 USA.

IEEE Log Number 9405273.

choose appropriate tracking. In short, the mathematical virtue is appropriateness; the processing virtues are efficiency and flexibility.

An alternative to m sequences is FM chirps. A large TW product is obtained by slowly sweeping the instantaneous frequency over a large operating range. This large TW basic signal can be repeated for an integer number of periods to form the desired transmission. The simplest FM signal is a linear chirp, with a constant amplitude and a linearly increasing instantaneous frequency. A linear chirp has an rms spectrum and a power spectrum that are both approximately rectangular, so its autocorrelation function (matched-filter output) is approximately sinc shaped, with a time resolution inversely proportional to its bandwidth, and the first sidelobe is approximately 13 dB below the main lobe. This sidelobe level usually does not meet the requirements for an application with long-range transmission and multipath or multimode reception. In order to shape the signal power spectrum so as to improve the sidelobe specification while maintaining an adequate time resolution, the FM chirp can be amplitude tapered [6]. The power spectrum of the tapered linear frequency modulated (TLFM) signal has the same shape as $A^2(t)$ except for some ripple errors, where $A(t)$ is the amplitude taper function.

Another way of obtaining a desirable output power spectrum is to use a nonlinear FM signal whose autocorrelation function has an acceptable main lobe width and a lower level of sidelobes. Since the autocorrelation function and the power spectrum are a Fourier transform pair, one can modify the autocorrelation function by properly shaping the signal power spectrum, that is, quickly moving through frequencies where the desired power spectrum is low and slowly moving through frequencies where the desired power spectrum is high. Nonlinear FM (NLFM) signals have been used extensively in radar [7]–[9], where the center frequency is usually very high, and the signal is considered a narrow-band signal.

It will be shown in this paper that, in applications involving long-range transmission of low-frequency acoustic energy over the ocean sound channel, an FM chirped signal with desirable properties can be realized such that the transmitted power is maximized by driving the transducer as hard as possible at each frequency. This is achieved by appropriately amplitude-modulating the FM chirp, so amplitude modulation cannot be used to shape the power spectrum as described in [6]. Shaping of the output power spectrum is achieved by using a nonlinear frequency modulation.

This paper discusses the design of a periodic signal using amplitude-modulated and nonlinear frequency-modulated (AM–NLFM) chirps, suitable for ocean acoustic travel-time measurements which require a good time resolution. The goal is to construct a signal with a desired output power spectrum, and capable of driving a given transducer to deliver maximum possible power into the ocean so that a long range transmission can be achieved. The designed signal is therefore system dependent. It will be shown that the signal can be formed either in the time domain or in the frequency domain. By forming the signal in the frequency domain, an output power spectrum identical to a prescribed shape without unwanted spectral ripples is attainable. Within the system bandwidth, this gives the signal designer full control over the signal's matched-filter output performance, namely, time resolution and sidelobe level specifications.

Section II describes the methodology behind the AM–NLFM signal design. Section III describes the signal design procedure. Section IV gives the waveforms and spectra of the designed signal, discusses the signal properties and its matched-filter performance, and compares the different design approaches. Section V concludes the paper.

II. Methodology

Consider a time-limited frequency-modulated signal:

$$s(t) = |s(t)| \exp[j\theta(t)], \qquad 0 \le t < T. \tag{1}$$

Its Fourier transform is

$$S(f) = |S(f)| \exp[j\Theta(f)]. \tag{2}$$

The signal to be designed is periodic with a period T. Let $s(t + iT)$ be its ith period.

The transducer, together with a cable and a tuner, can be modeled as a linear time-invariant system represented by a transfer function $H(f)$. Driving the system with a voltage $s(t)$ will yield an output sound pressure in the water $p(t)$ measured at 1 m from the transducer. The sound pressure spectrum $P(f)$ is related to $S(f)$ by

$$P(f) = H(f)S(f) \tag{3}$$

or

$$S(f) = H^{-1}(f)P(f). \tag{4}$$

We assume that 1) $s(t)$ is a unidirectional FM sweep and chirps upward, and 2) the magnitude $|s(t)|$ is slowly varying, and the rate of frequency sweep is low enough so that at any time t, the signal can be treated as a sinusoid having a frequency equal to the signal's instantaneous frequency f_i. The latter assumption is known as a quasi-steady-state (QSS) approximation [10]. Under the QSS assumption, the output sound pressure can be written as

$$p(t) = |H[f_i(t)]|\,|s(t)| \exp\{j\theta(t) + \arg[H(f_i(t))]\} \tag{5}$$

as if f_i were an eternal constant and $H[f_i(t)]$ a time-varying "gain" of the system. The reference cited showed that (5) is valid to a very high accuracy when the FM sweep rate in Hz/second is smaller than the square of the nominal bandwidth of $H(f)$, Hz^2.

Any real transducer will have certain physical constraints, such as a maximum allowable voltage across the ceramic stack and a maximum allowable stress in the stack. The cable between the power amplifier and the transducer may also have voltage and current limits (ATOC cables may be 10–100 km long). Taking into account all these constraints, one can find the maximum allowable input voltage. For a sinusoid with a frequency f, the input voltage limit is found by driving the system with the sinusoid and finding the amplitude B_f such that the most stringent limit within the linear system is reached. For a chirp, and under the QSS assumption, B_f

can be viewed as a function of the instantaneous frequency, denoted $B(f_i)$. Since the frequency sweeping is unidirectional, the instantaneous frequency $f_i(t)$ specifies a one-to-one relationship between time and instantaneous frequency. We now cast $B(f_i)$ into a function of time $B[f_i(T)]$, and let it be the signal magnitude:

$$s(t) = B[f_i(t)] \exp[j\theta(t)], \qquad 0 \le t < T. \tag{6}$$

The signal energy within an infinitesimal time interval δt is

$$\delta\mathcal{E}_t = |s(t)|^2 \delta t = B^2[f_i(t)]\delta t. \tag{7}$$

Meanwhile, consider an infinitesimal frequency range δf in the frequency domain. The signal energy within this range is

$$\delta\mathcal{E}_f = |S(f)|^2 \delta f = |H^{-1}(f)P(f)|^2 \delta f. \tag{8}$$

Our strategy is to combine (7) and (8) to form an equation to be used as the basis for developing the design procedure. However, the frequency arguments in (7) and (8) have different meanings. In (7), it is the instantaneous frequency, while in (8), it is a Fourier domain variable. Under the QSS assumption, f in $H(f)$ may be replaced with the instantaneous frequency. But replacing the argument of $P(f)$ with the instantaneous frequency will result in errors, which cannot be argued as negligible by the QSS assumption. In order to obtain a manageable design procedure, nevertheless, the instantaneous frequency f_i and the Fourier domain variable f will be used indiscriminately, denoted by f without a subscript. It is understood that this approximation will induce some errors, making the constructed signal depart from ideal. The effect of the induced errors will be discussed later.

By letting $\delta f = [df(t)/dt]\delta t$ where $df(t)/dt$ represents the instantaneous frequency sweeping rate, we can write the following expression from (7) and (8):

$$\frac{dt(f)}{df} = \frac{|H^{-1}(f)P(f)|^2}{B^2(f)} \tag{9}$$

where $t(f)$ is the inverse of $f(t)$, and is termed the group delay function. It is obtained by integration:

$$t(f) = \int_0^f \frac{|H^{-1}(\sigma)P(\sigma)|^2}{B^2(\sigma)} d\sigma. \tag{10}$$

Inverting $t(f)$, the instantaneous frequency function $f(t)$ is also found. The phase of the signal waveform $\theta(t)$ or the spectral angle in the frequency domain $\Theta(f)$ can be computed by integrating $f(t)$ or $t(f)$, respectively:

$$\theta(t) = 2\pi \int_0^t f(\tau) d\tau \tag{11}$$

$$\Theta(f) = -2\pi \int_0^f t(\sigma) d\sigma. \tag{12}$$

Having obtained $\theta(t)$ or $\Theta(f)$, the designed signal can be formed either in the time domain using (1)

$$s(t) = B[f(t)] \exp[j\theta(t)] \tag{13}$$

or in the frequency domain using (2)

$$S(f) = |H^{-1}(f)P(f)| \exp[j\Theta(f)]. \tag{14}$$

Bear in mind that the design is aimed at a signal with a prescribed time domain amplitude to meet the maximum power delivery requirement, and a prescribed frequency domain spectral magnitude to achieve a desirable time resolution and sidelobe levels at the receiver. However, both the time domain and frequency domain conditions cannot be strictly satisfied at the same time. A signal formed in the time domain with $|s(t)| = B[f(t)]$ perfectly conforms with the maximum input voltage constraints, but will have ripples in its spectrum. This is because, when using (13) to form the signal, the waveform envelope is made precisely equal to the desired shape, but the phase is computed from (11) originating from (9) which contains errors due to the indiscriminate use of f_i and f. This is similar, but not analogous, to the spectral ripples in the Fourier transform of a truncated time domain function. The spectral ripples will degrade the signal performance by effectively raising higher order sidelobe levels, as will be shown in the next section.

The frequency domain approach based upon (14), on the other hand, gives an output power spectrum perfectly in agreement with any desired shape, and hence a desirable matched-filter output at the receiver. But this will inevitably introduce ripples into $|s(t)|$ for the same reason spectral ripples are produced in the time domain approach. Ripples in the signal waveform envelope are likely to overshoot the function $B[f(t)]$, causing a violation of the system constraints. If this violation is intolerable, one must appropriately modify the signal magnitude function $B(f)$ used in computing $dt(f)/df$ [see (9)] in order to contain the peak of the time domain ripples within the system constraints. To achieve this, various parts of $B[f(t)]$ across the time axis are modified according to the extent to which the system constraints are overshot. The process can be carried out iteratively until a satisfactory result is achieved. The QSS assumption is used again as the modification of $B(f)$ is done at every instant *locally* across the time scale. The expense of such an operation is a slight reduction of the total transmitted energy. It should be noted that we cannot eliminate the waveform ripples in this way, but only reduce the peak of the ripples. In the next section, the frequency domain approach is described.

III. Signal Design

The purpose of the ATOC project is to monitor global temperatures attributed to the greenhouse effects. Reliably detecting the sound speed increase due to global warming requires a time resolution of about 0.05 s [11]. Also, a high signal-to-noise ratio and good multipath discrimination capability at the receiver are needed, requiring low sidelobe levels in the matched-filter output. The Pacific Ocean propagation set the signal period at roughly 30 s, with an overall duration about 20 min.

The motivation for this work, which provided the model to refine the design method and yielded the example results, was the first ATOC projector and associated system designed

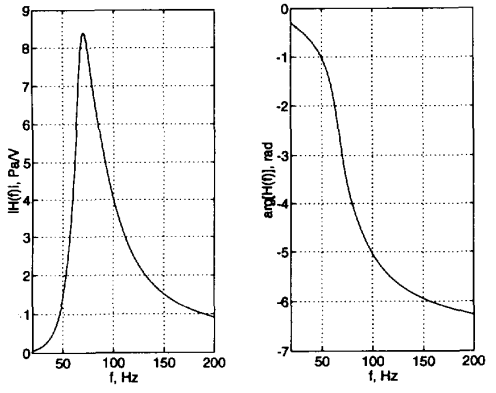

Fig. 1. System transfer function. (a) $|H(f)|$, (b) $\arg[H(f)]$.

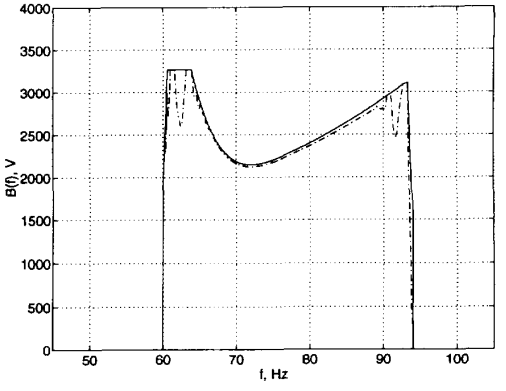

Fig. 2. Maximum allowable input voltage. Solid curve: initially computed. Dashed curve: modified.

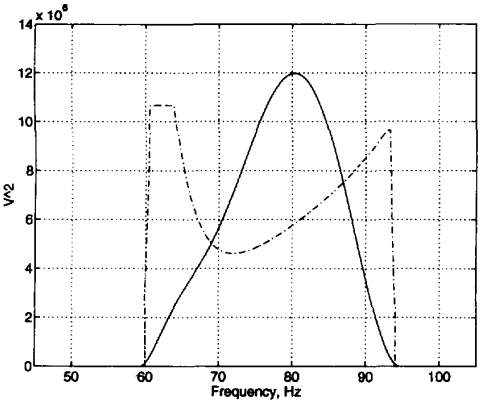

Fig. 3. $|S(f)|^2$ (solid) and $B^2(f)$ (dashed).

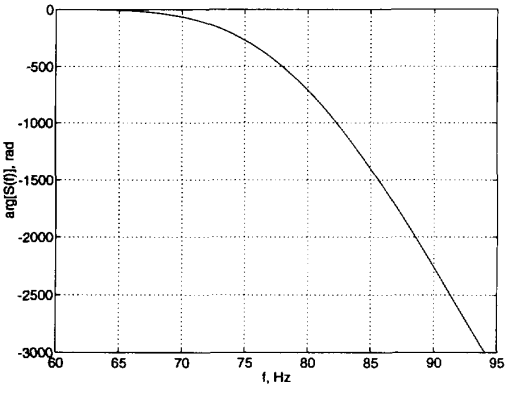

Fig. 4. Computed spectral angle.

and manufactured by Alliant Techsystems Inc., Mukilteo, WA. Alliant provided an electromechanical model of the projector and the input autotransformer, to which was added a model of 50 nmi of drive cable. The linearity of the projector and this detailed model of the system were the essential knowledge basis for our design. The details of the model are not included in this paper, which focuses on the design procedure and evaluation.

For completeness, we must mention that the ATOC workhorse signal will be based on m sequences and not FM. The two signals can yield similar resolution and power levels, but would be expected to have different Doppler behavior, and perhaps affect marine mammals differently.

The model used has a transfer function shown in Fig. 1. It is a bandpass system with a center frequency of 70 Hz. The projector has a CW capability of no less than 200 dB sound pressure level (SPL) referenced to 1 μPa at 1 m over an operating band of 60–94 Hz without violating the above-mentioned constraints.

In our numerical computation, a sampling frequency $f_s = 280$ Hz is used. The number of samples in a signal period is $N = 2^{13} = 8192$; therefore, each period is $T = 29\frac{9}{35} \approx 29.257$ s long. Each measurement will coherently analyze 40 consecutive periods.

When the system model is given and the physical constraints within the system are known, the maximum allowable input voltage as a function of frequency $B(f)$ can be computed based on the QSS assumption, as shown by the solid curve in Fig. 2.

To meet the time resolution and sidelobe level requirements, a cosine-squared spectrum is chosen as the desired output power spectrum. Taking the square root of the cosine-squared function gives the magnitude of the output pressure spectrum $|P(f)|$. Therefore, the magnitude of the desired voltage spectrum at the system input can be obtained by sending $|P(f)|$ backward through the linear system:

$$|S(f)| = |H^{-1}(f)|\,|P(f)|. \tag{15}$$

Having obtained $B(f)$ and $|S(f)|$, the derivative of the group delay function $dt(f)/df$ is the ratio of $|S(f)|^2$ and $B^2(f)$ (9). $|S(f)|^2$ (solid curve) and $B^2(f)$ (dashed curve) are shown in Fig. 3.

The spectral angle of the desired input signal $\Theta(f)$ can be found by first integrating $dt(f)/df$ over frequency to get $t(f)$, and then integrating $t(f)$ over f, as indicated by (10) and (12), respectively. Fig. 4 shows the computed $\Theta(f)$.

With both the magnitude and phase of the signal spectrum found, the input signal can be formed. Fig. 5(a) shows the

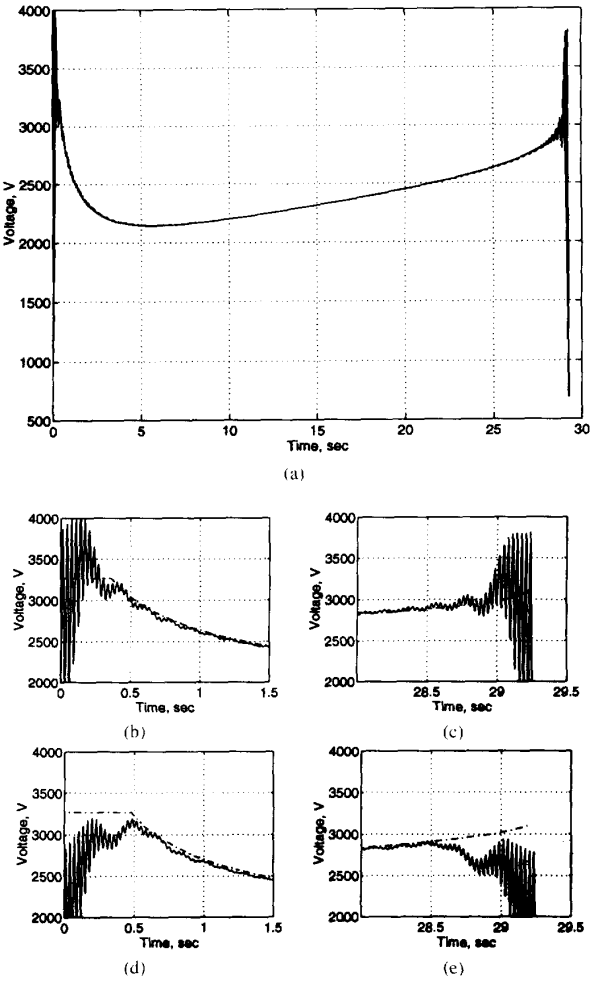

Fig. 5. Magnitude of signal waveform. (a) Waveform magnitude with time-domain ripples overshooting the system limit. (b), (c) Zoomed view of the waveform magnitude showing the overshooting. Dashed curves are $B[f(t)]$. (d), (e) Waveform magnitude without overshooting.

magnitude of the signal waveform in the time domain. This waveform has a desired cosine-squared power spectrum at the system output. As pointed out in Section II, the signal has time-domain ripples which overshoot the input voltage limit shown by the dashed curve in Fig. 5(b) and (c). Using the method explained in the previous section, a modified function $B(f)$ shown by the dashed curve in Fig. 2 is obtained. The modification results in an input signal waveform without overshooting, as shown in Fig. 5(d) and (e), conforming with the hardware constraints of the linear system.

As mentioned in the Introduction, the chirped signal segment will be transmitted repeatedly without a gap. At transitions between consecutive signal periods, the instantaneous phase $\theta(t)$ may have a discontinuity as shown in Fig. 6(a), causing an undesirable time-domain spike in the linear system. This can be remedied by slightly compressing or stretching the function $f(t)$ so that the instantaneous phase jump is

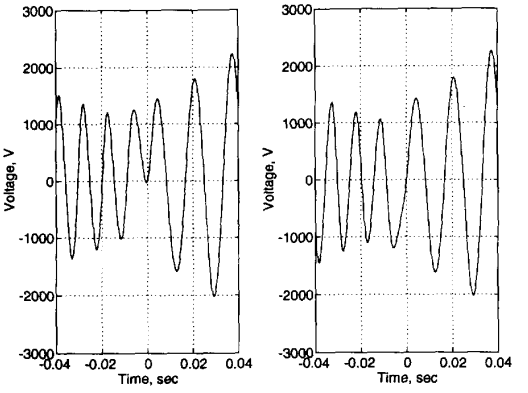

Fig. 6. Phase matching at transitions of consecutive periods. (a) With phase jump. (b) Phase continuous.

eliminated:

$$f_1(t) = \frac{2\pi \,\mathrm{round}[(\theta(T) - \theta(0))/(2\pi)]}{\theta(T) - \theta(0)} f(t) \qquad (16)$$

where T is the period of the signal segment, and the function round(x) rounds x toward the nearest integer. Inverting $f_1(t)$, a modified $t(f)$ is obtained, giving smooth transitions in the signal's instantaneous phase, as shown in Fig. 6(b). Thus, an AM nonlinear-FM input signal with smooth phase transition between adjacent periods is constructed in the frequency domain, which can drive the given transducer to produce maximum possible sound power into the ocean, and yield a sound pressure waveform at the system output with exactly the desired power spectral shape.

IV. Results and Discussion

A. Output Power Spectrum and Pressure Waveform

The design procedure described in Section III is based on the QSS assumption which must be validated by checking the resulting signal against the specifications and all the system constraints. Sending this signal through the system, and calculating voltage and current at various checkpoints within the system, as well as the stress in the ceramic stack, it is found that none of the system limitations is violated at any time. Using the frequency approach, an output power spectrum identical to the desired cosine-squared spectral shape is obtained, as shown in Fig. 7(a), where an arbitrary scale for the power spectra is used. The actual envelope of the waveform may be slightly lower than the dominant constraining limit due to the time domain ripple removal procedure [see Fig. 5(d), (e)]. This departure of the waveform envelope from the limit leads to a very small reduction of the total output power (on the order of 0.001 dB), which is practically negligible.

The smooth output power spectrum in Fig. 7(a) is compared to the rippled curve in Fig. 7(b), which is the output power spectrum produced by an input signal formed in the time domain, using the same $B(f)$ and $H(f)$. However, the time-domain formed signal has a smooth waveform envelope coincident with $B[f(t)]$, as shown in Fig. 8.

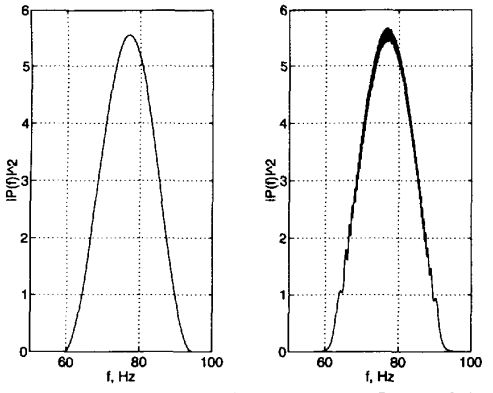

Fig. 7. Output power spectra (arbitrary scale). (a) Result of frequency domain approach. (b) Result of time domain approach.

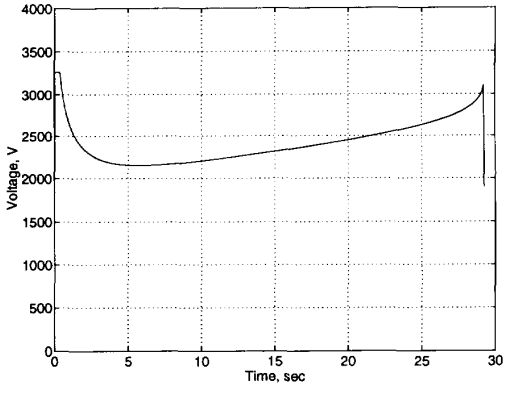

Fig. 8. Magnitude of the signal formed in the time domain.

Fig. 9 is the instantaneous output sound pressure level (SPL) measured at 1 m from the transducer and referenced to 1 μPa, obtained using the frequency domain approach. We define

$$\mathrm{SPL}_i = 10\log\left[\tfrac{1}{2}|p(t_i)|^2\right] + 120\,(\mathrm{dB}). \tag{17}$$

In (17), $p(t_i)$ is the sound pressure at 1 m in pascals, measured at the time t_i, $i = 1, \cdots, N$. It is seen that the SPL is over 200 dB and fairly even across the entire signal period. The average SPL is 201.5 dB, which is defined as

$$\overline{\mathrm{SPL}} = 10\log\left[\frac{1}{2N}\sum_{i=1}^{N}|p(t_i)|^2\right] + 120\,(\mathrm{dB}) \tag{18}$$

or

$$\overline{\mathrm{SPL}} = 10\log\left[\frac{1}{2N}\sum_{i=1}^{N}|p(f_i)|^2\right] + 120\,(\mathrm{dB}). \tag{19}$$

B. Matched-Filter Performance

Assuming an additive white Gaussian noise environment, the received signal can be matched filtered to yield a maximum signal-to-noise ratio. The matched-filter output is the autocorrelation function of the sound pressure waveform, the inverse Fourier transform of its power spectrum:

$$R(\tau) = \langle p(t)p^*(t-\tau)\rangle = \mathcal{F}^{-1}[|P(f)|^2]. \tag{20}$$

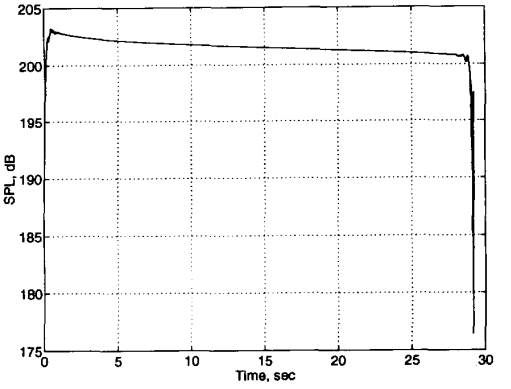

Fig. 9. Output sound pressure level (SPL) at 1 m, referenced to 1 μPa.

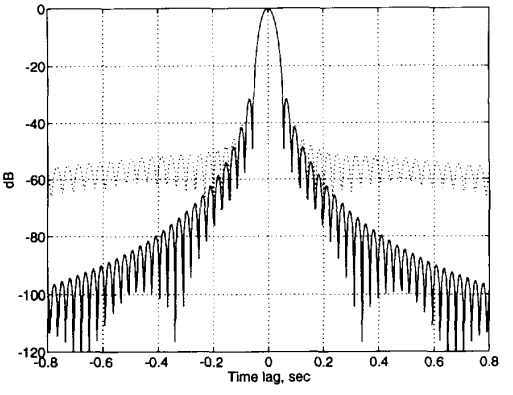

Fig. 10. Matched filter output. Solid: frequency domain approach, without spectral ripples. Dotted: Time domain approach, with spectral ripples.

For better time resolution, the signal can also be phase-only matched filtered by forming the filter with only the signal's spectral phase at the receiver [12]:

$$R_\phi(\tau) = \mathcal{F}^{-1}[P(f)\exp(-j\Phi(f))]. \tag{21}$$

$\Phi(f)$ is the phase of $P(f)$. Phase-only matched filtering causes all of the frequency components to add constructively at one moment of time. This is how a matched filter processes the spectral phase of the received signal. The output of this phase-only matched filter will have a better time resolution, but lower signal-to-noise ratio than phase and amplitude matched filtering. Phase and amplitude matched filtering is what is commonly and simply referred to as "matched filtering."

The solid curve in Fig. 10 shows the matched-filter output at the receiver. With a power spectrum identical to the desired cosine-squared shape, the time resolution measured at half the height of the main lobe maximum (−6 dB) is 0.056 s. The first sidelobe level is approximately 32 dB below the main lobe. At large time lags, the sidelobe levels are very low, and fall in a well-behaved manner without any undesirable irregularities.

The spectral ripples in the time-domain-formed signal have little effect on the main lobe. Therefore, the time resolution remains the same as the frequency domain approach result. But the higher order sidelobes are effectively raised, as shown by the dotted curve in Fig. 10.

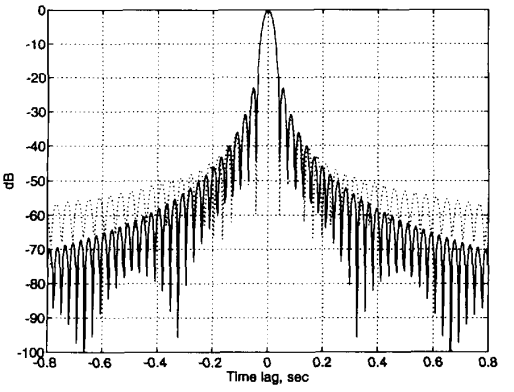

Fig. 11. Phase-only matched filter output. Solid: frequency domain approach, without spectral ripples. Dotted: Time domain approach, with spectral ripples.

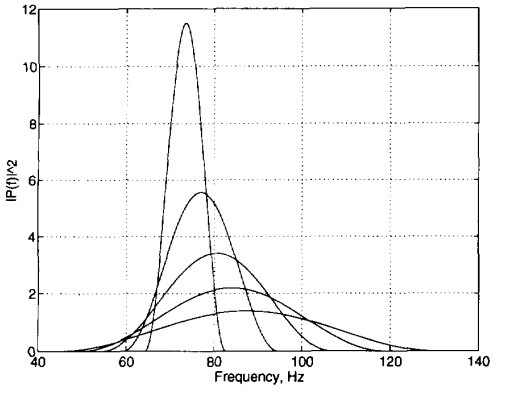

Fig. 12. Output power spectra with different operating bandwidths (arbitrary scale).

The solid curve in Fig. 11 is the phase-only matched-filter output. The time resolution is 0.045 s, better than the matched-filter output as expected. The improved time resolution is obtained at the cost of a higher level of sidelobes. The first sidelobe level is −23 dB, about 9 dB higher than the matched-filter result. The higher order sidelobes fall off in a well-behaved manner.

For a signal formed in the time domain, the spectral ripples do not have visible effects on the main lobe of the phase-only filter output, as in the case of matched filtering, but raise the sidelobe levels considerably. This is evident by observing the dotted curve in Fig. 11.

C. Output Power and Time Resolution Tradeoff

Time resolution is often the most critical specification in applications requiring precision arrival time measurement and good multipath discrimination; it is directly related to the signal bandwidth. In fact, if the transducer has more output power capability than is needed, one can "sell" some of the excess power capability for a better resolution. In other words, it is possible to chirp over a frequency range much wider than the system bandwidth to get a wider band signal in the water at a price of some output power reduction. As the frequency excursion is increased, the output energy is reduced because the signal frequency is farther from the "operating band" where the transducer can deliver its highest power. To demonstrate this effect, the design process was repeated for instantaneous frequency excursions other than the original 60–94 Hz excursion. The cosine-squared power spectrum was used for all excursions, so the 3 dB bandwidth is half the frequency excursion. For each excursion width, the center frequency was adjusted to obtain the maximum output power; Fig. 12 shows the power spectra used. The output average SPL and resolution results are given in Table I.

TABLE I
OUTPUT POWER/RESOLUTION TRADEOFF

band (Hz)	SPL (dB)	resolution (second)
65 - 82	201.9	0.109
60 - 94	201.6	0.056
55 - 106	201.2	0.038
50 - 118	200.5	0.029
45 - 130	199.5	0.023

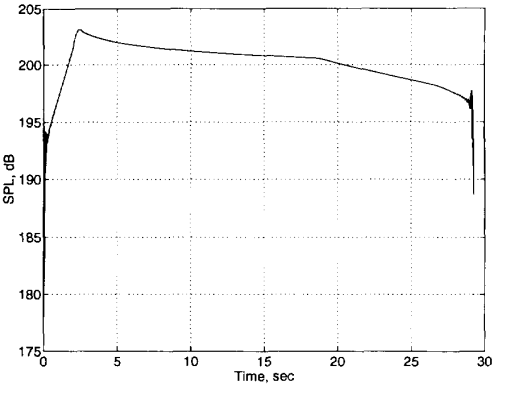

Fig. 13. Output SPL at 1 m, referenced to 1 μPa when using an operating frequency band of 50–118 Hz.

The time resolution is very close to 2 divided by the frequency excursion, i.e., close to the reciprocal of the 3 dB bandwidth. The surprise to the authors was that the decrease in output power was so little, about 1 dB to drive the resolution down to 29 ms, another dB for 23 ms. This was beyond the authors' expectation, and was gratifying since resolution is so essential in separating multiple arrivals.

The output power level becomes more variable across the chirp when the excursion is widened, as shown in Fig. 13 where an excursion of 50–118 Hz is used. The range of the SPL does not affect the matched-filter performance as it is the total transmitted signal energy that counts.

D. Results of Different Desired Spectral Shapes

The design procedure described in this paper is general, and any chosen power spectrum is attainable as long as the signal is not required to chirp over too large a bandwidth in too short a time. A number of functions other than a cosine-squared function have been used as the desired power spectrum. These

include a rectangle, a triangle, the main lobe of a sinc function, and cosine raised to powers of 4 and 16, respectively, all with an operating frequency excursion of 60–94 Hz. The output average SPL ranged from 201.2 to 201.6 dB referenced to 1 μPa at 1 m in seawater. This consistency is because the transducer is always driven to its limit within the specified frequency excursion.

V. Conclusion

Using a frequency domain approach, an AM–NLFM signal is obtained which can drive a given transducer to its maximum capacity and produce an output sound pressure in the water with a power spectrum identical to a prescribed shape.

The frequency domain approach is recommended because it produces lower sidelobe levels than the time domain approach. In a multipath or multimode application, it is important to have signals with low sidelobe levels. The overshooting in the time domain waveform introduced by forming the signal in the frequency domain can be suppressed with a slight reduction of output power.

Some previous work found in radar literature dealt with spectral ripples by modifying matched-filter characteristics [13] or using a so-called reciprocal-ripple technique [7], [14]. The frequency domain method gives an exact desired output power spectrum, eliminating the need for derippling at the receiver.

One of the advantages of using AM–NLFM signals is the flexibility in choosing a different operating frequency range and a preferred output power spectral shape in order to achieve an acceptable power/resolution and resolution/sidelobe level tradeoff. The design procedure introduced in this paper is general, and can be used as a routine in an iterative program to find such a tradeoff, giving a signal which meets the specifications and makes full use of the transducer's maximum power capability as well as available frequency bandwidth.

The design procedure is based on the quasi-steady-state assumption. Since no system constraints were violated and the desired power spectrum is attainable, the use of the QSS approximation is validated.

References

[1] P. F. Worcester, B. D. Cornuelle, and R. C. Spindel, "A review of ocean acoustic tomography: 1987–1990," *Rev. Geophys.*, suppl., pp. 557–570, Apr. 1991.

[2] D. Behringer, T. Birdsall, M. Brown, B. Cornuelle, R. Heinmiller, R. Knox, K. Metzger, W. Munk, J. Spiesberger, R. Spindel, D. Webb, and P. Worcester, "A demonstration of ocean acoustic tomography," *Nature*, vol. 299, pp. 121–125, Sept. 1982.

[3] A. Baggeroer and W. Munk, "The Heard Island feasibility test," *Phys. Today*, pp. 22–30, Sept. 1992.

[4] J. L. Spiesberger and K. Metzger, "Basin-scale tomography: A new tool for studying weather and climate," *J. Geophys. Res.*, vol. 96, pp. 4869–4889, Mar. 1991.

[5] T. G. Birdsall and K. Metzger, Jr., "Factor inverse matched filtering," *J. Acoust. Soc. Amer.*, vol. 79, pp. 91–99, Jan. 1986.

[6] T. F. Duda, "Analysis of finite-duration wide-band frequency sweep signals for ocean tomography," *IEEE J. Oceanic Eng.*, vol. 18, pp. 87–94, Apr. 1993.

[7] M. B. N. Butler, "Radar applications of s.a.w. dispersive filters," *Proc. IEE*, vol. 127, part F, pp. 118–124, Apr. 1980.

[8] J. A. Johnston and A. C. Fairhead, "Waveform design and Doppler sensitivity analysis for nonlinear FM chirp pulses," *Proc. IEE*, vol. 133, part F, pp. 163–175, Apr. 1986.

[9] F. E. Nathanson, *Radar Design Principles*. New York: McGraw-Hill, 1991, pp. 624–632.

[10] H. W. Batten, R. A. Jorgensen, A. B. Macnee, and W. W. Peterson, "The response of a panoramic receiver to CW and pulse signals," Dep. Elec. Eng., Univ. Michigan, Ann Arbor, Tech. Rep. 3, 1952.

[11] W. Munk, "The sound of ocean warming," *The Sciences*, vol. 33, pp. 21–25, Sept./Oct. 1993.

[12] T. G. Birdsall, "On understanding the matched filter in the frequency domain," *IEEE Trans. Educ.*, vol. E-19, pp. 168–169, Nov. 1976.

[13] A. Johnston, "Improvement to a pulse compression radar matched filter," *Radio Electron. Eng.*, vol. 53, pp. 138–140, Apr. 1983.

[14] G. W. Judd, "Technique for realizing low time sidelobes in small compression ratio chirp waveforms," in *Proc. IEEE Ultrason. Symp.*, 1973, pp. 478–481.

Shuozhong Wang was born in Sichuan, China, on September 29, 1943. He received the B.S. degree in radio and electronics from Beijing University, Beijing, China, in 1966, and the Ph.D. degree in electronic and electrical engineering from the University of Birmingham, England, in 1982.

He worked in the electronics industry before 1978. From 1983 to 1985 he was with Shanghai Acoustics Laboratory under the Chinese Academy of Sciences as a Research Fellow. Since 1985 he has been an Associate Professor at Shanghai University of Technology, China. At present, he is a Visiting Associate Research Scientist at the University of Michigan, Ann Arbor. His primary fields of study are underwater acoustics, signal processing, and digital image processing. His recent research topics include underwater acoustic signal design, ocean internal wave modeling, acoustic wave diffraction and scattering, and ultrasonic image processing.

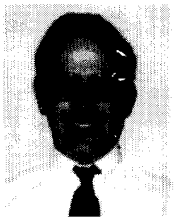

Mark L. Grabb (S'94) was born in Portsmouth, VA, on February 25, 1964. He received the B.S. degree in electrical engineering from North Carolina State University, Raleigh, in 1986, and the M.S. degree in electrical engineering from the University of Virginia, Charlottesville, in 1988.

He worked for the Defense Communications Agency and the Sperry Corporation during the summers of 1984–86. He worked for TASC, Reston, VA, from 1988 to 1992 in the area of communications and signal processing. Since 1992 he has been working toward the Ph.D. degree in electrical engineering at the University of Michigan. His interests are in signal processing and communication theory, with applications in long-range underwater sound propagation.

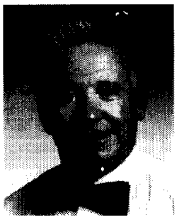

Theordore G. Birdsall (M'57–LM'93) received the B.S.E. degree, the M.S. degree in mathematics, and the Ph.D. degree in communication sciences.

He is a Professor in the Department of Electrical Engineering and Computer Science, University of Michigan, Ann Arbor. He has worked in engineering research since 1951, and has been on the teaching faculty since 1967. His primary interest is in the extraction of information from noisy signals, and his research has ranged from signal detection theory, through human hearing, radar, sonar, and spread spectrum communications to long-range underwater acoustic propagation, ocean acoustic tomography, and acoustic monitoring of ocean processes.